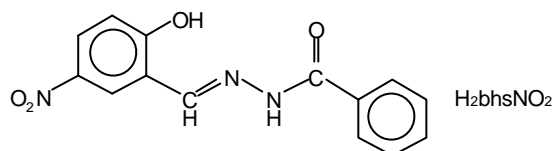


for studying the effect of amide protonation state on the coordination geometry, molecular structure, redox properties and interaction between the metal ions³. In the following account, the results obtained in our study on copper(II) chemistry with these two types of aroylhydrazones are summarized.

2. Bisphenoxo bridged dicopper(II) complex

In a dicopper(II) complex with **I**, either the phenolate-O or the deprotonated amide-O can bridge the metal ions. In such a situation, it has been observed earlier that the most negatively charged centre acts as the bridging atom⁴. Although dinuclear copper(II) complexes with this type of aroylhydrazones are reported earlier⁵, the identity of the bridging atom in these complexes is not unambiguous. We have been successful in growing single crystals of a dicopper(II) complex with H₂bhsNO₂ having the molecular



formula [Cu₂(bhsNO₂)₂(H₂O)₂]⁶. The complex has been synthesized by the reaction of Cu(O₂CCH₃)₂·H₂O and H₂bhsNO₂ (1:1 mole ratio) in methanol. The molecular structure of the complex is shown in figure 1. In solid state, the molecule has a crystallographically imposed inversion symmetry. The copper(II) centres are square-pyramidal. The amide-O, the imine-N and the bridging phenolate-O centres constitute the square bases and the apical sites are occupied by O-atoms of two water molecules.

Cryomagnetic measurements indicate that an antiferromagnetic interaction is operative between the two metal centres in [Cu₂(bhsNO₂)₂(H₂O)₂]. The least-squares fit of the magnetic data using an expression⁷ derived from the isotropic spin Hamiltonian, $H = -2JS_1 \cdot S_2$ ($S_1 = S_2 = 1/2$) provided a value of $-186(5) \text{ cm}^{-1}$ for the coupling constant J . The values of $2J$ observed for previously reported⁸ bisphenoxo bridged complexes are in the range -722 to -857 cm^{-1} . In such dicopper(II) complexes, the extent of antiferromagnetic interaction is known to decrease primarily due to: (i) decrease in the Cu–O–Cu bridge

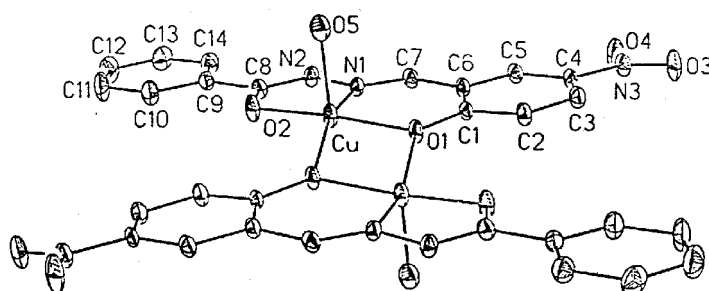


Figure 1. Molecular structure of [Cu₂(bhsNO₂)₂(H₂O)₂]. Hydrogen atoms are omitted for clarity.

angle, (ii) increase in the pyramidal character of the bridging O-atom, and (iii) tetrahedral distortion of the square base containing the metal centre⁸. In $[\text{Cu}_2(\text{bhsNO}_2)_2(\text{H}_2\text{O})_2]$, the bridging phenolate-O atoms are planar (solid angle 359.6°). However, the Cu atom is displaced by 0.24 \AA from the mean basal plane towards the apical water O-atom. In addition, the average deviation of O1 and O2 from the mean basal plane is 0.11 \AA and that of N1 and symmetry related phenolate-O is -0.11 \AA . Thus the lowering of the J value in the present complex compared to that of the other similar species is possibly due to the distortion of the coordination geometry around the metal centre, relatively smaller Cu–O–Cu bridge angle (100.4°) and the presence of electron withdrawing nitro group⁹ at the para position of the bridging phenolate-O.

3. Protonation of the amide functionalities in $[\text{Cu}_2(\text{bhsNO}_2)_2(\text{H}_2\text{O})_2]$

To explore the effect of amide protonation state on the properties of $[\text{Cu}_2(\text{bhsNO}_2)_2(\text{H}_2\text{O})_2]$, we have tried to protonate the coordinated amide functionalities by adding stoichiometric quantity of HClO_4 to the acetonitrile solution of the complex. In this attempt, a square-pyramidal monomeric copper(II) complex, $[\text{Cu}(\text{HbhsNO}_2)(\text{CH}_3\text{CN})_2]\text{ClO}_4$ has been isolated¹⁰. The solid state molecular structure of the complex has been determined by X-ray crystallography. The bond parameters associated with the metal ion and other physical properties are consistent with the +2 oxidation state of the metal ion. Intraligand bond parameters clearly suggest the protonation of the amide functionality. The mononegative planar ligand coordinates the metal ion via the phenolate-O, the imine-N and the O-atom of the protonated amide functionality. The N-atom of one of the two acetonitrile molecules completes the square base and that of the other acetonitrile molecule satisfies the apical position (figure 2). The Cu-atom is displaced by 0.23 \AA out of the mean basal plane in the direction of the apical acetonitrile N-atom. The equatorial acetonitrile molecule is bound to the metal ion more strongly (Cu–N4, $1.946(3) \text{ \AA}$) compared to the apical acetonitrile in a reasonably linear fashion (Cu–N4–C15,

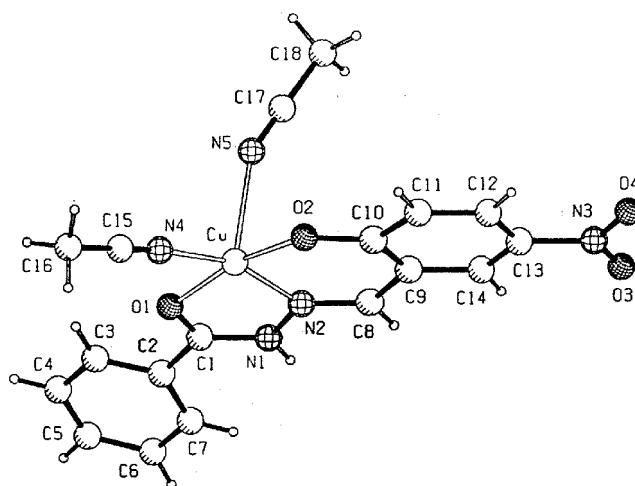
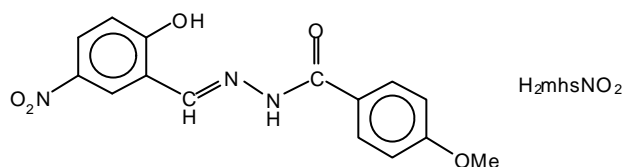


Figure 2. Structure of $[\text{Cu}(\text{HbhsNO}_2)(\text{CH}_3\text{CN})_2]^+$ and the atom labelling scheme.

172.9(3)°). However, the apical acetonitrile molecule (Cu-N5, 2.387(3) Å) is in a very rare bent mode (Cu-N5-C17, 154.6(3)°). In structurally characterized adducts of nitriles¹¹, the observed deviations of the M–N≡C bond angle from 180° are within 8° for monodentate nitriles and that for chelating dinitriles are within 11°. To the best of our knowledge, the only other known example containing a similar bent monodentate nitrile is SmI₂(NCCMe₃)₂ (Sm–N≡C, 151.3(6)°)¹².

In order to examine whether the copper(II) coordination geometry can be influenced by an electron releasing substituent on the aryl fragment of the ligand, another Schiff base, viz. H₂mhsNO₂, has been used to synthesize a similar acetonitrile coordinated mono-



nuclear copper(II) complex. The molecular formula of the isolated complex is [Cu(HmhsNO₂)(CH₃CN)(ClO₄)]¹⁰. Figure 3 depicts the molecular structure of this complex determined by X-ray crystallography. The bond parameters and other physical properties suggest the presence of protonated amide functionality in HmhsNO₂[−] and also the +2 oxidation state of the metal ion in this complex. The coordination geometry around the metal centre is again square-pyramidal. The tridentate O,N,O-donor ligand and the acetonitrile-N constitute the basal plane. However, in contrast to the previous complex a perchlorate O-atom (Cu-O6, 2.564(2) Å) occupies the apical position and there is no displacement (0.007 Å) of the metal centre towards apical coordinating atom. In this complex, the equatorial acetonitrile molecule (Cu-N4, 1.965(2) Å; Cu-N4-C16, 177.6(2)°) is unexceptional.

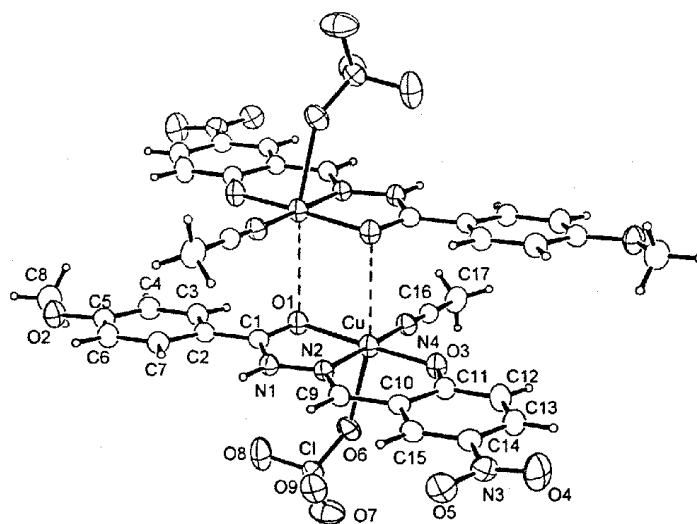


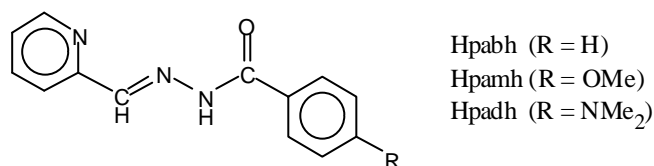
Figure 3. Molecular structure of [Cu(HmhsNO₂)(CH₃CN)(ClO₄)] and the dimeric arrangement of the molecules via weak Cu...O interactions.

The shortest Cu...Cu distance in the crystal lattice of this molecule is 3.835(1) Å. Interestingly this is due to formation of dimeric aggregates via the amide-O of the protonated amide functionalities. Two [Cu(HmhsNO₂)(CH₃CN)(ClO₄)] molecules are involved in a pair of complementary very weak interactions between the metal ions and the amide-O centres (Cu'...O1, 2.909(2) Å, Cu'...O1-Cu, 101.77(9)°) at the sites trans to the apical perchlorate-O atom (figure 3). This weak interaction may be partially responsible for not observing the displacement of the Cu-atom from the basal plane towards the perchlorate-O atom.

4. Complexes with 2-pyridine-carboxaldehyde aroylhydrazones

4.1 Mononuclear hexacoordinated copper(II) complexes

In hexacoordinated copper(II) complexes, tetragonal distortion from the octahedral symmetry due to the Jahn–Teller distortion is very common. Such complexes with different ligands are attractive mainly due to the variation in the coordination geometry and the spectral features^{13,14}. Schiff bases (**II**) derived from 2-pyridine-carboxaldehyde and aroylhydrazines provide the pyridine-N, the imine-N and the amide-O as the metal coordinating atoms and form two five-membered chelate rings upon complexation with a metal ion. Two of such deprotonated meridionally spanning ligands produce a neutral copper(II) complex containing a CuN₄O₂ coordination sphere. In methanolic media, reactions of one mole of Cu(O₂CCH₃)₂·H₂O and two moles of HL (Hpabh, Hpamh



and Hpadh) in methanol afford the complexes of general formula CuL₂ in moderate to high yield¹⁵. The *S* = 1/2 spin state in each complex is confirmed by room temperature (298 K) magnetic moments (1.90–2.08 *m*_B). The electronic spectral features are comparable with those of other similar hexacoordinated copper(II) complexes. X-ray crystal structure of [Cu(pabh)₂] has been determined (figure 4). Intraligand distances are in conformity with the enolate form of both the ligands. Interestingly the two ligands are inequivalent in terms of metal to coordinating atom distances. For the first ligand the distances are: Cu-N1, 2.130(3) Å; Cu-N2, 1.940(3) Å; Cu-O1, 2.099(2) Å and for the second ligand the distances are: Cu-N4, 2.286(3) Å; Cu-N5, 1.972(3) Å; Cu-O2, 2.294(3) Å. These distances clearly suggest a tetragonal elongation along the O2-Cu-N4 axis. The average of Cu-N(imine) distances is 1.956 Å and that of Cu-O1 and Cu-N1 distances is 2.114 Å. These two values indicate a tetragonal compression along the N2-Cu-N5 axis. Such a compression is not unexpected considering the rigidity of these tridentate ligands¹⁴. Thus the CuN₄O₂ coordination sphere in [Cu(pabh)₂] is rhombically distorted. This fact is further supported by the EPR results as described below.

Room temperature (298 K) powder EPR spectral profiles of all the three complexes (figure 5) display an interesting trend. Three signals observed for [Cu(pabh)₂] are in complete agreement with the rhombic distortion of the CuN₄O₂ coordination sphere as found in the solid state structure. At low temperature such rhombic spectra are reported

for hexacoordinated copper(II) complexes of meridionally spanning tridentate ligands¹⁴. In the spectrum of $[\text{Cu}(\text{pamh})_2]$, g_1 is observed as a shoulder on g_2 indicating lesser rhombicity of the N_4O_2 sphere compared to that in $[\text{Cu}(\text{pabh})_2]$. On the other hand, $[\text{Cu}(\text{padh})_2]$ displays a broad asymmetric signal near $g=2$ (figure 5) indicating a

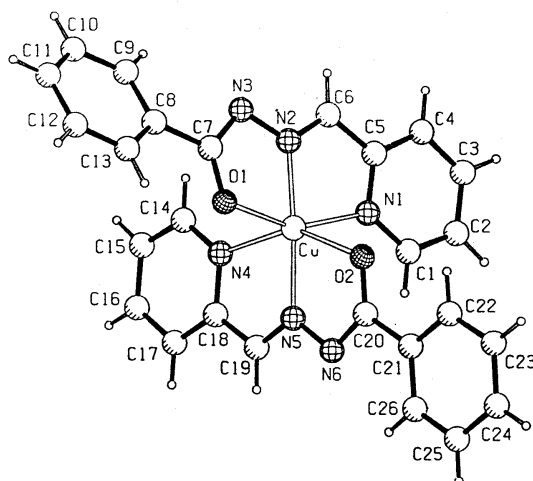


Figure 4. Molecular structure of $[\text{Cu}(\text{pabh})_2]$ with the atom labelling scheme.

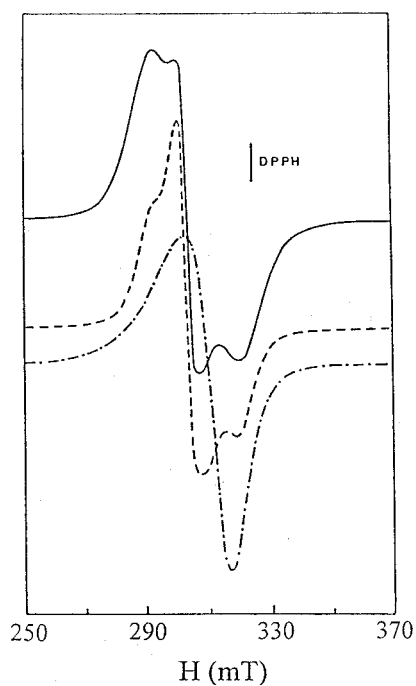


Figure 5. Powder EPR spectra (at 298 K) of $[\text{Cu}(\text{pabh})_2]$ (—), $[\text{Cu}(\text{pamh})_2]$ (---) and $[\text{Cu}(\text{padh})_2]$ (-·-·-).

tetragonal elongation rather than a rhombic distortion. A possible rationale for this gradual transition from rhombic to tetragonally elongated N_4O_2 sphere around copper(II) in these complexes is as follows. In the structure of $[Cu(pabh)_2]$, two ends of one ligand sit on the Jahn–Teller elongated axis. The imine-N of this ligand and the other three coordinating atoms of the second ligand constitute the square-plane. In this $N_{\text{imine}}O_{\text{amide}}N_{\text{imine}}N_{\text{pyridine}}$ square-plane the average of Cu– N_{imine} bond distances is smaller than that of the Cu– N_{pyridine} and Cu– O_{amide} bond distances. The electron donating ability of the substituent at the para position of the aroyl fragment decreases in the order $padh^- > pamh^- > pabh^-$. Therefore the Cu– O_{amide} bond strength is expected to decrease in the order $[Cu(padh)_2] > [Cu(pamh)_2] > [Cu(pabh)_2]$ and hence the Cu– O_{amide} bond distance decreases in the reverse order. As a result, the difference between the average of the Cu– N_{imine} bond distances and that of Cu– N_{pyridine} and Cu– O_{amide} bond distances decrease in the following order: $[Cu(pabh)_2] > [Cu(pamh)_2] > [Cu(padh)_2]$. Thus between $[Cu(pabh)_2]$ and $[Cu(pamh)_2]$, the former displays a larger rhombicity than the latter in the EPR spectrum. The near axial spectrum of $[Cu(padh)_2]$ indicates similar metal to coordinating atom distances in the $N_{\text{imine}}O_{\text{amide}}N_{\text{imine}}N_{\text{pyridine}}$ square-plane.

4.2 Dimeric and polymeric copper(II) complexes

The tridentate deprotonated Schiff bases of type **II** are expected to provide the O-atom of the amide functionality as the bridging atom in a dicopper(II) complex. In search of such a complex, we have used all the three Schiff bases (HL = Hpabh, Hpamh and Hpadh) described in the previous section. The observations for Hpadh are quite different from that for Hpabh and Hpamh. The results obtained with the latter two Schiff bases are described in this section.

In methanolic media, reactions of $Cu(O_2CCH_3)_2 \cdot H_2O$ and HL (in 1:1 mole ratio) afford complexes having empirical formulae $CuL(O_2CCH_3)$ and that of $CuCl_2 \cdot 2H_2O$, HL and KOH (in 1:1:1 mole ratio) provide complexes having empirical formulae $CuLCl$ ¹⁶. IR spectra of the complexes indicate deprotonation of the amide functionality in HL. The powder EPR spectral profiles of the complexes are very similar and typical of a square-planar or square-pyramidal copper(II) complex. The g_{\parallel} and g_{\perp} values are observed in the ranges 2.26–2.33 and 2.09–2.19 respectively. Electronic spectral features of these complexes in methanol solutions are also consistent with a square-planar or square-pyramidal copper(II) complex. In methanol solutions, all the complexes are found to be redox active. Cyclic voltammograms of $Cu(pabh)(O_2CCH_3)$ and $Cu(pamh)(O_2CCH_3)$ display Cu(II)/Cu(I) reductions at –0.29 and –0.22 V, respectively and those of $Cu(pabh)Cl$ and $Cu(pamh)Cl$ display the reductions at –0.07 and –0.06 V (vs Ag/AgCl), respectively. Considering the higher basicity of acetate-O compared to that of chloride the more anodic potentials observed for the chloride containing complexes is not surprising.

X-ray crystal structures of all the four complexes have been determined. In each complex, the planar tridentate monoanionic ligand coordinates the metal ion via the pyridine-N, the imine-N and the amide-O atom of the deprotonated amide functionality. The fourth site is occupied by the acetate-O or chloride to form a square-plane around the metal centre.

In the solid state, both $Cu(pabh)(O_2CCH_3)$ and $Cu(pamh)(O_2CCH_3)$ exist as centrosymmetric dimeric species with the acetate groups acting as monoatomic equatorial-apical bridges¹⁶. Thus the metal centres of $[Cu_2(\mu-O_2CCH_3)_2L_2]$ are in

distorted square-pyramidal N_2O_3 coordination spheres. For both complexes the bond parameters in the O,N,N,O basal plane are unexceptional. The Cu-O(apical) distance is relatively larger (2.284 Å) and the Cu-atom is displaced towards the apical bridging acetate O-atom by ~ 0.1 Å. The Cu...Cu distances are identical in both complexes. These are: 3.273(2) Å ($L^- = \text{pabh}^-$) and 3.273(1) Å ($L^- = \text{pamh}^-$). The Cu-O-Cu bridge angles are: $101.4(2)^\circ$ ($L^- = \text{pabh}^-$) and $101.94(15)^\circ$ ($L^- = \text{pamh}^-$).

An interesting observation in the structures of these two diacetato bridged complexes is the distances between the uncoordinated acetate O-atoms and the azomethine ($-\text{HC}=\text{N}-$) carbon atoms of the adjacent dimers. These O...C distances are 3.162(10) Å and 3.199(6) Å for $[\text{Cu}_2(\text{mO}_2\text{CCH}_3)_2(\text{pabh})_2]$ and $[\text{Cu}_2(\text{mO}_2\text{CCH}_3)_2(\text{pamh})_2]$, respectively. The corresponding C-H...O angles are 140.2 and 142.9° . Thus in each case, a one-dimensional assembly of the dinuclear molecule is formed by the involvement of the molecule in two pairs of reciprocal C-H...O interactions with its two neighbours on both sides (figure 6). The interdimer Cu...Cu distances for $[\text{Cu}_2(\text{mO}_2\text{CCH}_3)_2(\text{pabh})_2]$ and $[\text{Cu}_2(\text{mO}_2\text{CCH}_3)_2(\text{pamh})_2]$ are 5.818(3) and 5.652(2) Å, respectively.

In the solid state, magnetic moment (per Cu) of each of these two acetato bridged complexes at 300 K is $\sim 1.9 \mu_B$. On cooling (up to 17 K), no significant change in the magnetic moments is observed for both complexes. Linear relationships of the inverse magnetic susceptibilities with temperature clearly indicate that both complexes behave as Curie paramagnets (figure 7). The Curie (C) and Weiss (θ) constants obtained by fitting the data using the expression for Curie-Weiss law are 0.45 and -1.41 K and 0.46 and -1.04 K for the complexes of pabh^- and pamh^- , respectively. Very small spin coupling constants J (-1.54 to $+0.63 \text{ cm}^{-1}$) have been reported for other similar acetato bridged dicopper(II) complexes^{16,17}. The small values of θ observed for the present complexes suggest a similar situation in these two complexes.

X-ray structures show that in each of the two chloride containing complexes, the metal centre is in a distorted square-pyramidal N_2OCl_2 coordination sphere (figure 8). As is the case with the acetate containing complexes described above, $\text{Cu}(\text{pabh})\text{Cl}$ is also a centrosymmetric equatorial-apical dichloro bridged dinuclear species (figure 8a). However, $\text{Cu}(\text{pamh})\text{Cl}$ exists as polymeric chain species via equatorial-apical chloride bridges (figure 8b)¹⁶. The bond parameters in the N,N,O,Cl basal plane are unexceptional for a copper(II) species. Like most square-pyramidal species, the metal centre is displaced towards the apical Cl-atom by 0.23 Å in the dimeric complex and by 0.13 Å in the polymeric complex. The Cu-Cl(apical) distance (2.6682(10) Å) in the dimeric

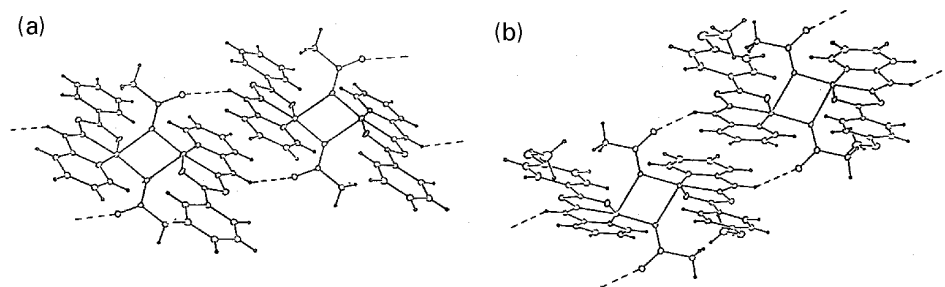


Figure 6. One-dimensional ordering of (a) $[\text{Cu}_2(\text{mO}_2\text{CCH}_3)_2(\text{pabh})_2]$, and (b) $[\text{Cu}_2(\text{mO}_2\text{CCH}_3)_2(\text{pamh})_2]$ via C-H...O interactions.

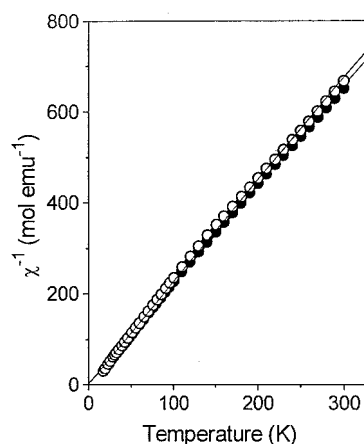


Figure 7. Temperature dependence of inverse magnetic susceptibilities (per monomer) for $[\text{Cu}_2(\mathbf{m}\text{-O}_2\text{CCH}_3)_2(\text{pabh})_2]$ (O) and $[\text{Cu}_2(\mathbf{m}\text{-O}_2\text{CCH}_3)_2(\text{pamh})_2]$ (●). The solid lines represent the Curie-Weiss law fits.

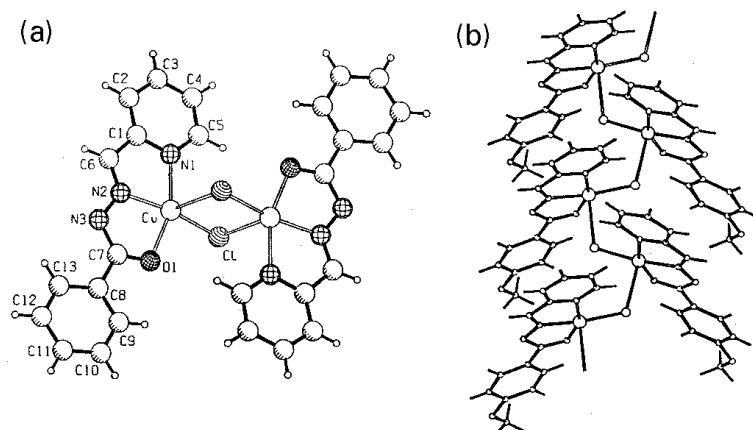


Figure 8. (a) Molecular structure of $[\text{Cu}_2(\mathbf{m}\text{-Cl})_2(\text{pabh})_2]$ with the atom labelling scheme. (b) Single chloride bridged one-dimensional structure of $[\text{Cu}(\text{pamh})\text{Cl}]_n$.

complex is noticeably shorter than that (2.7821(13) Å) in the polymeric species. The Cu...Cu distances and the Cu-Cl-Cu bridge angles are 3.3918(9) Å and 86.89(3)° and 4.2866(7) Å and 117.60(5)° for the dimeric and polymeric species, respectively.

Variable temperature magnetic susceptibility data indicate the Curie paramagnetic behaviour for both $[\text{Cu}_2(\mathbf{m}\text{-Cl})_2(\text{pabh})_2]$ and $[\text{Cu}(\text{pamh})\text{Cl}]_n$. The C and q values obtained by linear least-squares fits of the data are 0.45 and -3.57 K and 0.42 and 1.98 K for $[\text{Cu}_2(\mathbf{m}\text{-Cl})_2(\text{pabh})_2]$ and $[\text{Cu}(\text{pamh})\text{Cl}]_n$ respectively. Magnetostructural correlations for equatorial-apical dichloro bridged copper(II) dimeric complexes have been reported earlier¹⁸. The spin-exchange coupling constant J in this type of complexes have been found in the range -41.3 to +6 cm⁻¹. An empirical relationship has been established with the extent of spin-spin interaction and the ratio f/R (where f is the Cu-Cl-Cu bridge

angle and R is the Cu–Cl (apical) distance). As this ratio increases, the value of $-2J$ decreases and reaches a minimum and then again increases. For the complexes having $fR \approx 33$ the value of J is minimal. The paramagnetic behaviour of $[\text{Cu}_2(\mathbf{m}\text{Cl})_2(\text{pabh})_2]$ is consistent with the value (32.6) of fR in this complex.

Cryomagnetic behaviour of very few single chloride bridged polymeric copper(II) complexes are reported¹⁹. The intrachain magnetic interaction is very weak. The value of J is in the range -6.1 to 1.58 cm^{-1} . However, a trend in the Cu–Cl–Cu bridge angle (f) and the coupling constant J has been observed¹⁹. The value of J is negative (-6.1 cm^{-1}) for large f (144.6°). On the other hand, species with small f display a weak ferromagnetic character ($f=128.1^\circ$, $J=0.48 \text{ cm}^{-1}$; $f=113.58^\circ$, $J=1.58 \text{ cm}^{-1}$). The small but positive Weiss constant (1.98 K) observed for $[\text{Cu}(\text{pamh})\text{Cl}]_n$ suggests an essentially paramagnetic character of the complex. However, it is interesting to note that f ($117.60(5)^\circ$) in $[\text{Cu}(\text{pamh})\text{Cl}]_n$ is intermediate of the two f values in those weakly ferromagnetic species.

4.3 Copper(II) assisted transformation of azomethine to imidate

Anticipating that a better electron releasing group such as $-\text{NMe}_2$ at the para position of the aroyl fragment of **II** may help in obtaining a deprotonated amide-O bridged dicopper(II) species, reaction of $\text{Cu}(\text{O}_2\text{CCH}_3)_2 \cdot \text{H}_2\text{O}$ and Hpadh (1:1 mole ratio) in methanol has been conducted. X-ray crystal structure determination of the isolated product reveals that instead of the desired dicopper(II) complex, a centrosymmetric dimeric diacetato bridged complex has been produced. As in the case of acetate containing complexes described in the previous section, the acetate groups act as monoatomic equatorial-apical bridges between the copper(II) centres in this complex. However, the azomethine group ($-\text{HC}=\text{N}-$) of Hpadh is transformed to imidate ($-(\text{OMe})\text{C}=\text{N}-$) in the complexed ligand (padh'^-)²⁰. The molecular structure $[\text{Cu}_2(\mathbf{m}\text{O}_2\text{CCH}_3)_2(\text{padh}')_2]$ is depicted in figure 9a. The free Schiff base (Hpadh) has been prepared in methanol and can be recrystallized from the same solvent. The molecular structure of Hpadh determined by X-ray crystallography is shown in figure 9b. Thus it is clear that the azomethine to imidate transformation in Hpadh occurs only after

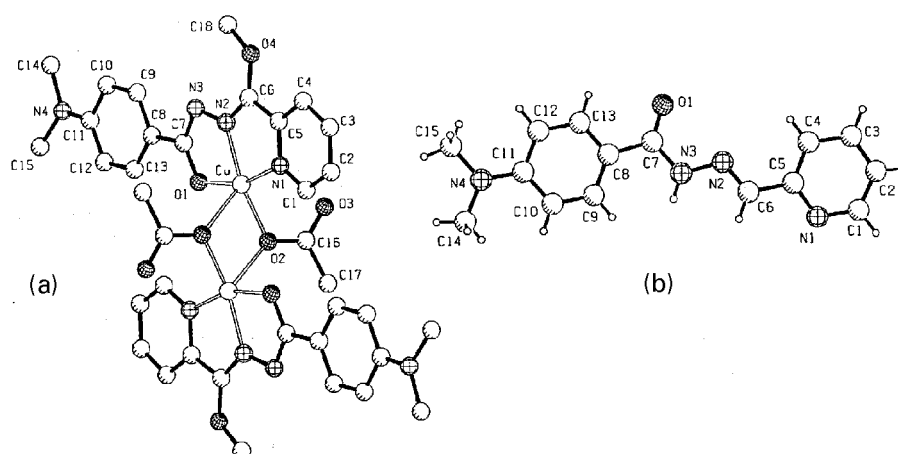
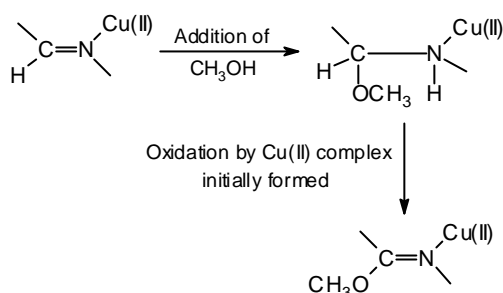
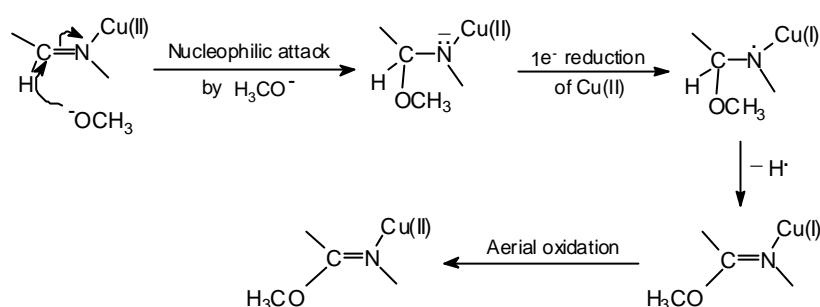


Figure 9. Molecular structures of (a) $[\text{Cu}_2(\mathbf{m}\text{O}_2\text{CCH}_3)_2(\text{padh}')_2]$ and (b) Hpadh.



Scheme 1.



Scheme 2.

complexation with copper(II). It is expected that the azomethine group will be more polarized due to metal ion coordination to the imine-N. At least two pathways can be proposed for the observed transformation of the azomethine group. These are: (i) addition of methanol to the polarized azomethine moiety followed by oxidation to the isolated product $[\text{Cu}_2(\text{mO}_2\text{CCH}_3)_2(\text{padh}')_2]$ by a portion of the copper(II) complex initially formed (scheme 1) and (ii) a nucleophilic attack at the polarized azomethine carbon by a methoxide followed by reduction of copper(II) to copper(I), homolytic cleavage of (OMe)C–H bond to form (OMe)C=N and finally oxidation of the metal ion from +1 state to +2 state by aerial oxygen (scheme 2). The low yield (31%) of $[\text{Cu}_2(\text{mO}_2\text{CCH}_3)_2(\text{padh}')_2]$ with respect to total copper taken during synthesis supports mechanism (i). Addition of water or alcohol to a metal coordinated azomethine group has been observed earlier²¹. A mechanism similar to (i) has been suggested for the conversion of coordinated azomethine to amide in presence of water²².

4.4 Self-assembly of $[\text{Cu}(\text{Hpadh})\text{Cl}_2]$ via hydrogen bonding and *p-p* interaction

The reaction of Hpadh, $\text{CuCl}_2 \cdot 2\text{H}_2\text{O}$ and KOH (1:1:1 mole ratio) in methanol has been performed expecting the isolation of a chloride containing complex analogous to that described in §4.2. However, the amide functionality remains protonated in the isolated complex, $[\text{Cu}(\text{Hpadh})\text{Cl}_2]$. This possibly happens due to the lower acidity of the amide proton in Hpadh caused by the presence of the strong electron releasing NMe_2 group at the para position of the aroyl fragment. The same complex has been isolated from methanolic medium in good yield (72%) by reacting Hpadh and $\text{CuCl}_2 \cdot 2\text{H}_2\text{O}$ in absence

of KOH. The bond parameters obtained from the X-ray crystal structure determination and all other physical properties are consistent with the protonated amide functionality and the +2 oxidation state of the metal ion in this complex²³. The molecule has a square-pyramidal structure. The planar tridentate Hpadh coordinating through the pyridine-N,

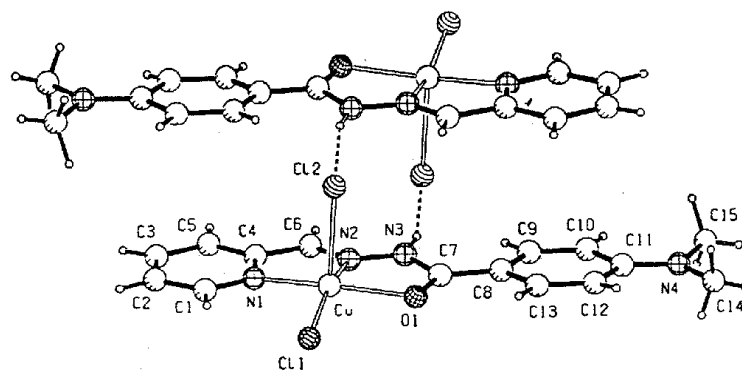


Figure 10. Hydrogen bonded dimeric arrangement of $[\text{Cu}(\text{Hpadh})\text{Cl}_2]$ molecules.

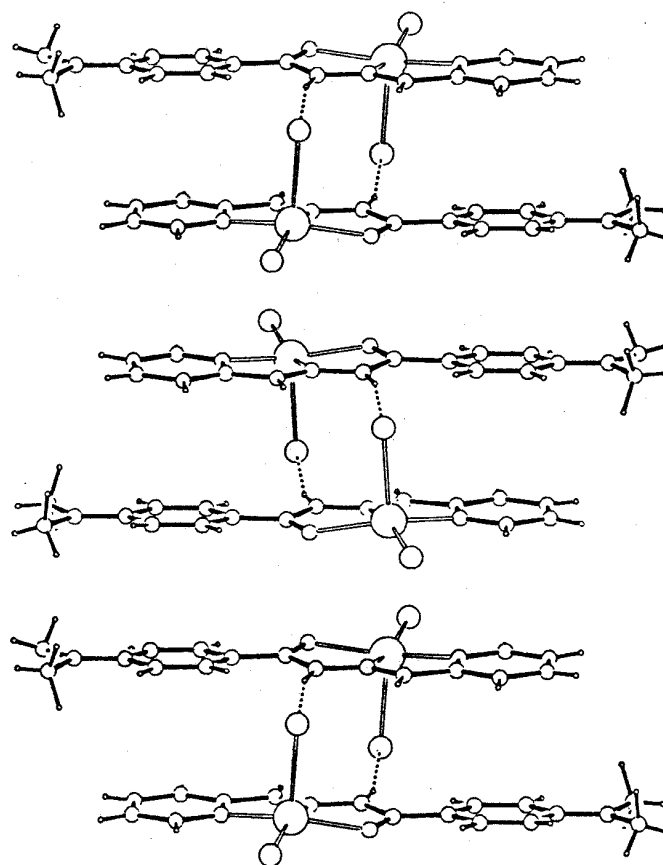


Figure 11. One-dimensional assembly of $[\text{Cu}(\text{Hpadh})\text{Cl}_2]$ molecules through N-H...Cl hydrogen bonds and *p-p* interactions.

the imine-N and the amide-O and one of the two chloride ions form the square base. The remaining chloride occupies the apical site. The metal to coordinating atom distances in the basal plane are comparable with those observed for the other similar complexes described in the previous sections. The Cu–Cl(apical) distance (2.5128(10) Å) is significantly longer than the Cu–Cl(equatorial) distance (2.2053(9) Å). As observed in most square-pyramidal complexes, the copper atom is displaced by 0.274 Å from the basal plane towards the apical chlorine in this complex. Two [Cu(Hpadh)Cl₂] molecules are involved in a pair of reciprocal hydrogen bonds between the amide hydrogen atoms and the apical chlorine atoms (figure 10). The N...Cl distance is 3.080 Å and the N–H...Cl angle is 162.4°. In this hydrogen bonded dimeric unit, the Cu...Cu distance is 6.455 Å. The ligand aromatic rings of [Cu(Hpadh)Cl₂] units in each hydrogen bonded dimer are involved in **p-p** interactions with the aromatic rings of adjacent dimers. The interplanar distances between the overlapping aroyl moiety rings and the pyridine rings are 3.578 and 3.534 Å, respectively. The corresponding centroid-to-centroid distances are 3.754 and 4.246 Å, respectively. Thus the pyridine rings are more slipped compared to the aroyl benzene rings. In the dimeric fragment formed by the **p-p** interactions, the Cu...Cu distance is 4.023 Å. Thus in the solid state, a one-dimensional assembly of [Cu(Hpadh)Cl₂] molecules with alternate long and short Cu...Cu distances is formed through sequential intermolecular N–H...Cl hydrogen bonds and **p-p** interactions (figure 11).

Due to the short Cu...Cu distance between the **p**stacked hydrogen bonded dimers, we have attempted a detailed investigation of the magnetic behaviour of this complex. However, variable temperature magnetic susceptibility data collected by using a powdered sample of [Cu(Hpadh)Cl₂]_n suggest no significant spin-spin interaction between the metal ions. The data could be satisfactorily fit using the expression for the Curie–Weiss law. The Curie and Weiss constants obtained are 0.454(1) and –0.8(3) K, respectively.

5. Concluding remarks

We have explored the coordination chemistry of copper(II) with aroylhydrazones with a specific aim of synthesizing amide-O bridged dicopper(II) complexes. Although we were unable to isolate such a species, several interesting monomeric, dimeric and polymeric complexes could be synthesized in the course of our investigation. The influence of electronic nature of the ligand substituents on the subtle variation of the coordination geometry in hexacoordinated copper(II) complexes has been noted. A rare example of a copper(II) complex containing a unidentate bent acetonitrile has been characterized. Metal ion activated transformation of azomethine to imidate has been realised for the first time. In the solid state, weak intermolecular interactions such as C–H...O and N–H...Cl hydrogen bonding and **p-p** interactions lead to interesting one-dimensional self-assembly of some of the complexes. At present, we are engaged in generating new supramolecular species of copper and other metal ion complexes with these Schiff bases and different ancillary ligands.

Acknowledgements

Financial support received from the Council of Scientific and Industrial Research, New Delhi is gratefully acknowledged. I am deeply indebted to my students and coworkers

whose names appear in the references. X-ray crystallographic studies were performed at the National Single Crystal Diffractometer Facility, School of Chemistry, University of Hyderabad (funded by the Department of Science and Technology, New Delhi).

References

1. (a) Hodgson D J 1975 *Prog. Inorg. Chem.* **19** 173; (b) Creutz C 1983 *Prog. Inorg. Chem.* **30** 1; (c) Kahn O 1985 *Angew. Chem., Int. Ed. Engl.* **24** 834
2. (a) Zanello P, Tamburini S, Vigato P A and Mazzocchin G A 1987 *Coord. Chem. Rev.* **77** 165; (b) Fenton D E 1983 *Advances in inorganic and bio-organic mechanisms* (ed.) A G Sykes (London: Academic Press) vol. 2, p. 187; (c) Fenton D E 1988 *Metal clusters in proteins* (ed.) L Que Jr (Washington, DC: ACS)
3. (a) Pal S N, Radhika K R and Pal S 2001 *Z. Anorg. Allg. Chem.* **627** 1631; (b) Sangeetha N R and Pal S 2000 *Bull. Chem. Soc. Jpn.* **73** 357; (c) Sangeetha N R and Pal S 1997 *J. Coord. Chem.* **42** 157; (d) Lakshmi A V, Sangeetha N R and Pal S 1997 *Indian J. Chem.* **A36** 844; (e) Sangeetha N R, Pal C K, Ghosh P and Pal S 1996 *J. Chem. Soc., Dalton Trans.* 3293
4. Sinn E 1976 *Inorg. Chem.* **15** 358
5. (a) Biradar N S and Havinale B R 1976 *Inorg. Chim. Acta* **17** 157; (b) Iskander M F, El-Aggan A M, Refaat L S and El Sayed L 1975 *Inorg. Chim. Acta* **14** 167
6. Sangeetha N R, Baradi K, Gupta R, Pal C K, Manivannan V and Pal S 1999 *Polyhedron* **18** 1425
7. O'Connor C J 1982 *Prog. Inorg. Chem.* **29** 203
8. (a) Mandal S K, Thompson L K, Newlands M J, Gabe E J and Nag K 1990 *Inorg. Chem.* **29** 1324; (b) Nag K 1990 *Proc. Indian Acad. Sci. (Chem. Sci.)* **102** 269
9. Hay P J, Thibeault J C and Hoffmann R 1975 *J. Am. Chem. Soc.* **97** 4884
10. Sangeetha N R and Pal S 1999 *J. Chem. Crystallogr.* **29** 287
11. (a) Storhoff B N and Takats J 1977 *Coord. Chem. Rev.* **23** 1 (b) Beatti I R, Jones P J, Howard J A K, Smart L E, Gilmore C J and Akitt J W 1979 *J. Chem. Soc., Dalton Trans.* 528; (c) Bombieri G, Benetollo F, Klahne E and Fischer R D 1983 *J. Chem. Soc., Dalton Trans.* 1115; (d) Blount J F, Freeman H C, Hemmerich P and Sigwart C 1969 *Acta Crystallogr.* **B25** 1518; (e) Gorter S and Veschoor G C 1976 *Acta Crystallogr.* **B32** 1704
12. Chebolu V, Whittle R R and Sen A 1985 *Inorg. Chem.* **24** 3082
13. (a) Reinen D and Friebel C 1979 *Struct. Bonding* **37** 1; (b) Hathaway B J 1984 *Struct. Bonding* **57** 55; (c) Hitchman M A, Maasicant W, van der Plas J, Simmons C J and Stratemeier H 1999 *J. Am. Chem. Soc.* **121** 1488
14. (a) Storrier G D, Colbran S B and Craig D C 1997 *J. Chem. Soc., Dalton Trans.* 3011; (b) Folgado J V, Henke W, Allman R, Stratemeier H, Beltran-Porter D, Rojo T and Reinen D 1990 *Inorg. Chem.* **29** 2035; (c) Blake A J, Lavery A J and Schroder M 1996 *Acta Crystallogr.* **C52** 37
15. Pal S N, Pushparaju J, Sangeetha N R and Pal S 2000 *Transition Met. Chem.* **25** 529
16. Sangeetha N R and Pal S 2000 *Polyhedron* **19** 1593
17. Chiari B, Helms J J, Piovesana O, Tarantelli T and Zanazzi P F 1986 *Inorg. Chem.* **25** 870
18. (a) Rojo T, Arriortua M I, Ruiz J, Darriet J, Villeneuve G and Beltran-Porter D 1987 *J. Chem. Soc., Dalton Trans.* 285; (b) Marsh W E, Patel K C, Hatfield W E and Hodgson D J 1983 *Inorg. Chem.* **22** 511
19. Estes W E, Hatfield W E, van Ooijen J A C and Reedijk J 1980 *J. Chem. Soc., Dalton Trans.* 2121
20. Sangeetha N R, Pal S N and Pal S 2000 *Polyhedron* **19** 2713
21. (a) Busch D H and Bailar J C Jr. 1956 *J. Am. Chem. Soc.* **78** 1137; (b) Harris C M and McKenzie E D 1962 *Nature (London)* **196** 670
22. Menon M, Choudhury S, Pramanik A, Deb A K, Chandra S K, Bag N, Goswami S and Chakravorty A 1994 *J. Chem. Soc., Chem. Commun.* 57
23. Sangeetha N R, Pal S N, Anson C E, Powell A K and Pal S 2000 *Inorg. Chem. Commun.* **3** 415